Parameter Forecasts From CMB Lensing and Galaxy Lensing Power- and Bispectra

Jonas Frugte[1] and **P. Daniel Meerburg**[2]

[1]Independent Researcher, The Netherlands
[2]Van Swinderen Institute for Particle Physics and Gravity, University of Groningen, Nijenborgh 4, 9747 AG Groningen, The Netherlands

E-mail: jonasfrugte@gmail.com

May 8, 2025

NB: Currently still in draft.

Abstract

1 Introduction

Weak lensing has been used as a probe to constrain cosmological parameters since the 2000's [18, 3, 16, 26, 5]. A range of upcoming surveys, such as the survey by the Simons Observatory (SO) [1], the Legacy Survey of Space and Time (LSST) [14], and Euclid [19] aim to measure weak lensing of the CMB and of galaxies. They will do so much more accurately than previous surveys, enabling tighter constraints on parameters and progressing our understanding of physics as a whole. Typically, the main value of interest is the power spectrum (or equivalently, two point function) of the lensing potential. This can be measured in terms of the lensing convergence κ, lensing shear γ, or lensing potential ψ. In the weak lensing regime they all contain the same amount of information and can be easily converted into one another, see section B. For the CMB the lensing potential is generally measured directly [23], while with galaxies one instead measures the shear, as this can be deduced from the ellipiticity distribution of the observed galaxies [13].

Even with Gaussian initial conditions, there are significant amounts of non-Gaussianity in the weak lensing signal, especially in galaxy lensing due to it being a probe of the more recent distribution of matter [6, 24]. In addition to looking at the power spectrum, a natural next step is thus to measure the lensing bispectrum. This has already been done for signals from galaxies [27], but no proper detection has been done of the CMB lensing bispectrum. Upcoming surveys such as the ones mentioned earlier may detect this signal. Therefore it is relevant to know the detectability of, and parameter constraints possible from, all 4 signals: CMB lensing power- and bispectra and galaxy lensing power- and bispectra. Notably, this includes looking at cross correlation as well.

In this article we aim to answer this question in the context of experimental parameters similar to those of next generation surveys such as mentioned earlier. We are especially interested in seeing if approximate parameter degeneracies can be broken by combining all data. Calculating the covariance matrix of unbiased optimal estimators of the cosmological parameters can be done by combining cosmological simulations (in our case we use the CAMB package [20]) with a Fisher matrix analysis. See figure 1 for an overview of the calculation done in this paper. The parameters looked at are the Hubble constant, H_0, physical baryon density, $\Omega_b h^2$, physical cold dark matter density, $\Omega_c h^2$, scalar spectral index, n_s, amplitude of primordial scalar fluctuations, A_s, sum of neutrino masses $\sum m_\nu$, and dark energy equation of state parameter, w_0. Though, we will find that some of the parameters are poorly constrained even when combining all 4 signals and thus omit them from the analysis in the results. As a secondary purpose, this paper also includes a derivation for the Fisher matrix formalism in the non-trivial context of bispectra with multiple tracers. The final formula can already be found in the literature (see e.g. the appendix of [17]), but the authors of this paper were not able to find a derivation and hence included it.

The structure of this paper is as follows: we first review the theory of weak lensing and weak lensing statistics in sections A and B. We then provide technical details of the calculation in section 3, such as choices for noise and numerical approximations made in the code. In section 4 we present the results, consisting of signal to noise ratios and parameter constraints for different combinations of the CMB and galaxy lensing power- and bispectra. We conclude in section 5. Appendix C contains a short review of the Fisher matrix formalism and gives a technical derivation of the formula used to calculate each Fisher matrix element in the case of bispectra measurements with multiple tracers. Finally, appendix D explains how to relate the shear to the lensing potential in spherical harmonic space.

All code written for this project is uploaded on github at `https://github.com/Jonas-Frugte/fisher_calc_weak_lensing`.

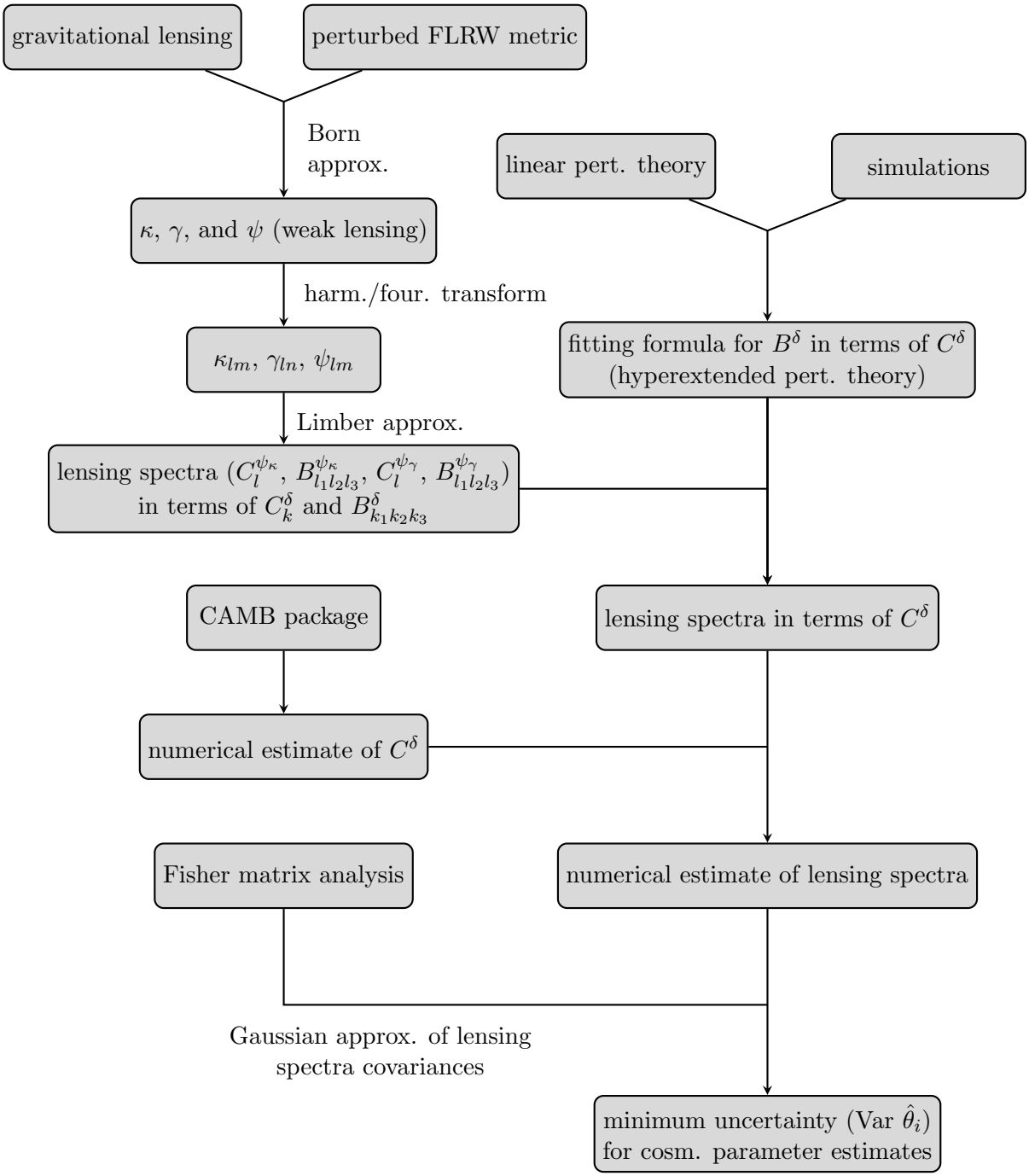

Figure 1: Flowchart of steps involved in calculating the minimum error/uncertainty in cosmological parameter estimates using convergence and shear power- and bi-spectra.

2 Theory

2.1 Weak lensing spectra

Radiation from cosmological objects is distorted due to gravitational lensing. In the vast majority of cases this lensing is a relatively weak effect and is thus referred to as weak lensing. Weak lensing is quantified through the deflection field $\mathbf{d}(\hat{\mathbf{n}})$ which equals the difference between the observed angle of a point on the sky and the true (unlensed) angle. This field is the gradient of the lensing potential $\psi(\hat{\mathbf{n}})$ given as a weighted integral over the mass distribution along the line of sight between earth and the observed point.

In the case of CMB surveys, lensing alters the statistical properties of the temperature and polarization fields and can thus be calculated by comparing to the expected unlensed signal, see e.g. [21]. In galaxy surveys, lensing alters the ellipiticities of observed galaxies. If a large enough number of galaxies are observed, this effect can be seperated from the intrinsic ellipiticities of the galaxies and thus the lensing potential can be estimated.

To constrain cosmological parameters we can then look at the lensing potential of the CMB, ψ_{CMB}, and of galaxy surveys, ψ_{gal}. These are directly related to the matter power and bispectra as

$$\begin{aligned} C_l^{\psi_X\psi_Y} &= \frac{9}{l^4}\Omega_m^2 H_0^4 \int_0^{\chi_*} \chi^2 \mathrm{d}\chi a(\eta_0-\chi)^{-2} W_X(\chi) W_Y(\chi) C^\delta(l/\chi, \eta_0-\chi), \\ B_{l_1 l_2 l_3}^{\psi_X\psi_Y\psi_Z} &= \sqrt{\frac{(2l_1+1)(2l_2+1)(2l_3+1)}{4\pi}} \begin{pmatrix} l_1 & l_2 & l_3 \\ 0 & 0 & 0 \end{pmatrix} \frac{27}{l_1^2 l_2^2 l_3^2}\Omega_m^3 H_0^6 \\ &\quad \times \int \chi^2 \mathrm{d}\chi a(\eta_0-\chi)^{-3} W_X(\chi) W_Y(\chi) W_Z(\chi) B^\delta(\{l_i/\chi\}, \eta_0-\chi), \end{aligned}$$

with $X, Y, Z \in \{\text{CMB}, \text{gal}\}$. Ω_m is the present day matter density parameter, H_0 is the present day Hubble constant, $a(\eta)$ is the scale factor, η_0 is the conformal time today, χ is the comoving radial distance, χ_* the distance to surface of last scattering, $P^\delta(k, \eta)$ the matter power spectrum, $B^\delta(k_1, k_2, k_3, \eta)$ the matter bispectrum, $W_X(\chi)$ the window function, and

$$\begin{pmatrix} l_1 & l_2 & l_3 \\ m_1 & m_2 & m_3 \end{pmatrix}$$

the Wigner 3-j symbol. The only factor that differs between CMB and galaxy lensing is the window function, defined as

$$W_X(\chi) = \int_\chi^\infty \mathrm{d}\chi' p_X(\chi') \frac{\chi' - \chi}{\chi'\chi},$$

with p_X the radius distribution of the radiation source. For the CMB we take $p(\chi) = \delta(\chi - \chi_*)$. Notice that we can also look at cross correlation between CMB and galaxy lensing.

For a derivation of the lensing potential and its power- and bispectra, see appendices A and B.

2.2 Nonlinear matter bispectrum

Determining the nonlinear matter powerspectrum can be done using numerical codes such as CAMB. The nonlinear matter bispectrum was calculated from the powerspectrum using a fitting formula based on perturbation theory in [12]. It is given by

$$B^{\delta}(k_1, k_2, k_3, \chi) = 2F_2(k_1, k_2, z)C^{\delta}(k_1, z)C^{\delta}(k_2, z) + 2 \text{ perm.} \tag{1}$$

where C^{δ} is the nonlinear matter power spectrum[1], and the kernel F_2 is modified from the tree level result with factors $a(k, z)$, $b(k, z)$, and $c(k, z)$:

$$F_2(k_1, k_2, z) = \frac{5}{7}a(k_1, z)a(k_2, z) + \frac{k_1^2 + k_2^2}{2k_1k_2}b(k_1, z)b(k_2, z)\cos\theta + \frac{2}{7}c(k_1, z)c(k_2, z)\cos^2\theta. \tag{2}$$

They are defined as:

$$a(k, z) = \frac{1 + \sigma_8^{a_6}(z)\sqrt{0.7}Q(n_{\text{eff}})(q^{a_1})^{n_{\text{eff}}+a_2}}{1 + (q^{a_1})^{n_{\text{eff}}+a_2}}, \tag{3}$$

$$b(k, z) = \frac{1 + 0.2a_3(n_{\text{eff}} + 3)(q^{a_7})^{n_{\text{eff}}+3+a_8}}{1 + (q^{a_5})^{n_{\text{eff}}+3.5+a_8}}, \tag{4}$$

$$c(k, z) = \frac{1 + \left[\frac{4.5a_4}{1.5+(n_{\text{eff}}+3)^4}\right](q^{a_5})^{n_{\text{eff}}+3+a_9}}{1 + (q^{a_5})^{n_{\text{eff}}+3.5+a_9}}. \tag{5}$$

Here, $Q(n_{\text{eff}})$ is given by:

$$Q(x) = \frac{4 - 2x}{1 + 2^{x+1}}. \tag{6}$$

The effective spectral index of the linear power spectrum is defined as:

$$n_{\text{eff}} \equiv \frac{d\ln C_{\text{lin}}^{\delta}(k)}{d\ln k}. \tag{7}$$

Additionally, q is given by:

$$q = \frac{k}{k_{\text{NL}}}, \tag{8}$$

where k_{NL} is the scale at which nonlinearities become significant, satisfying:

$$4\pi k_{\text{NL}}^3 C_{\text{lin}}^{\delta}(k_{\text{NL}}, 0) = 1. \tag{9}$$

The coefficients a_i are:

$$a_1 = 0.484, \quad a_2 = 3.740, \quad a_3 = -0.849, \quad a_4 = 0.392,$$
$$a_5 = 1.013, \quad a_6 = -0.575, \quad a_7 = 0.128, \quad a_8 = -0.722, \quad a_9 = -0.926.$$

[1]Compare to the tree level bispectrum where we instead use the linear powerspectrum.

2.3 Fisher matrix analysis

SNR and parameter constraints are obtained through a Fisher matrix analysis as is standard. A full derivation of below statements can be found in appendix C. The auto and cross power spectrum Fisher matrix is given as

$$F_{\alpha\beta} = \sum_l \sum_{XY} \sum_{X'Y'} (2l+1) \partial_\alpha C_l^{XY} (C^{-1})_l^{XX'} (C^{-1})_l^{YY'} \partial_\beta C_l^{X'Y'}$$

where

$$C_l := \begin{pmatrix} C_l^{\psi_\kappa \psi_\kappa} & C_l^{\psi_\kappa \psi_\gamma} \\ C_l^{\psi_\kappa \psi_\gamma} & C_l^{\psi_\gamma \psi_\gamma} \end{pmatrix}.$$

For the bispectra we instead get

$$F_{\alpha\beta} = \sum_{l_1 \leq l_2 \leq l_3} \frac{\mathcal{P}_{l_1 l_2 l_3}}{6} \sum_{XYZ} \sum_{X'Y'Z'} \partial_\alpha B_{l_1 l_2 l_3}^{XYZ} (C^{-1})_{l_1}^{XX'} (C^{-1})_{l_2}^{YY'} (C^{-1})_{l_3}^{ZZ'} \partial_\beta B_{l_1 l_2 l_3}^{X'Y'Z'},$$

with $\mathcal{P}_{l_1 l_2 l_3}$ defined as the number of distinct permutations that can be made with $l_1 l_2 l_3$. When only considering autospectra the formulas simplify to

$$F_{\alpha\beta} = \sum_l \sum_{XY} \sum_{X'Y'} \frac{2l+1}{2} \frac{\partial_\alpha C_l^{XX} \partial_\beta C_l^{XX}}{(C_l^{XX})^2},$$

and (for bispectra)

$$F_{\alpha\beta} = \sum_{l_1 \leq l_2 \leq l_3} \frac{\mathcal{P}_{l_1 l_2 l_3}}{6} \frac{\partial_\alpha B_{l_1 l_2 l_3}^{XXX} \partial_\beta B_{l_1 l_2 l_3}^{XXX}}{C_{l_1}^{XX} C_{l_2}^{XX} C_{l_3}^{XX}}.$$

3 Calculation Details

We chose our fiducial cosmology in line with the results from the Planck mission [2].

$$\begin{aligned}
H_0 &= 67.4\,\text{km/s/Mpc}, && \text{(Hubble constant)} \\
\Omega_b h^2 &= 0.0223, && \text{(Physical baryon density parameter)} \\
\Omega_c h^2 &= 0.119, && \text{(Physical cold dark matter density parameter)} \\
n_s &= 0.965, && \text{(Scalar spectral index)} \\
A_s &= 2.13 \times 10^{-9}, && \text{(Amplitude of primordial scalar fluctuations)} \\
\sum m_\nu &= 0.06\,\text{eV}, && \text{(Sum of neutrino masses)} \\
w_0 &= -1. && \text{(Dark energy equation of state parameter)}
\end{aligned}$$

This paper considers noise levels for stage 3 and stage 4 weak lensing surveys. Values can be found in table 1. A comparison of noise power spectrum to lensing power spectrum can be found in figure 2.

CMB noise is estimated through the quadratic estimator developed in [21]. We do not take temperature measurements into account, as these are subleading for stage 4 experiments (REF). This

source	survey stage	noise vals	comparable experiments
CMB	stage 3	$\sigma = 1'$, $\Delta_P = 6'$ μK	Advanced ACTPol, SPT-3G
	stage 4	$\sigma = 3'$, $\Delta_P = 1'$ μK	CMB-S4, LiteBIRD
galaxies	stage 3	$\sigma_{\rm rms} = 0.3$, $n_g = 5 \text{arcmin}^{-2}$	DES, KiDS
	stage 4	$\sigma_{\rm rms} = 0.3$, $n_g = 30 \text{arcmin}^{-2}$	LSST, Euclid

Table 1: Noise levels considered for weak lensing of galaxies and the CMB. σ (beam width) and Δ_P (polarization white noise) describe CMB survey specifications, while $\sigma_{\rm rms}$ (intrinsic galaxy ellipticity) and n_g (observed galaxy density) refer to galaxy shear surveys.

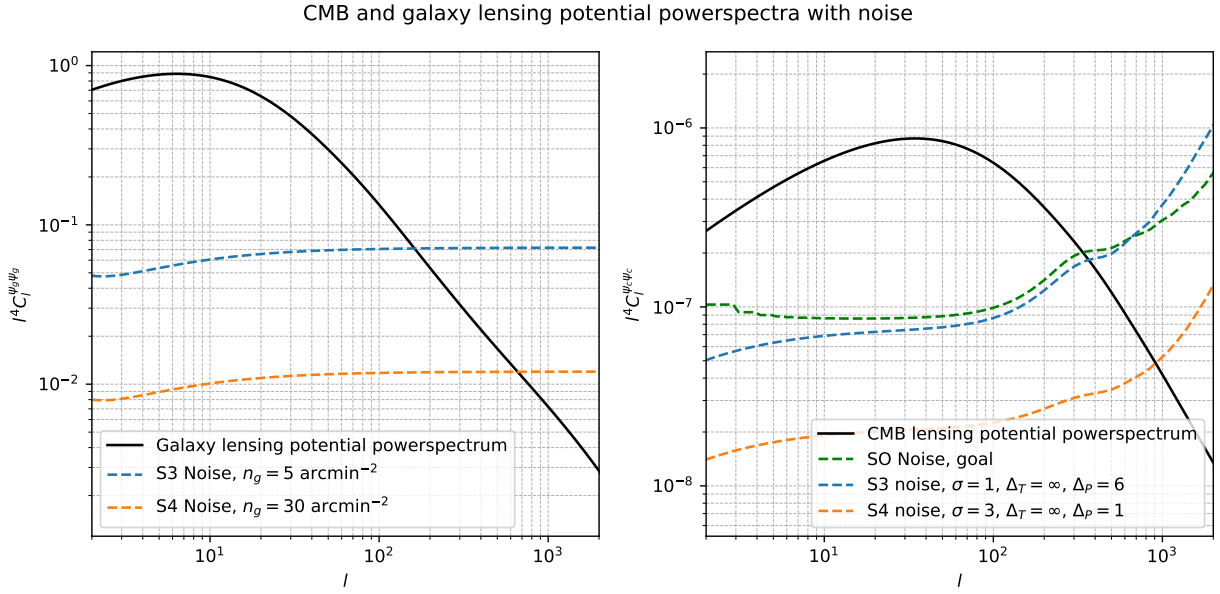

Figure 2: CMB (right) and galaxy (left) lensing potential power spectra compared to associated experimental noise. Current (stage 3) noise values are displayed as well as near future (stage 4) noi se values. The CMB lensing experiment does not measure temperature anisotropies, only polarization. CMB noise values are chosen in accordance with [22]. Shear noise values are chosen to be similar to e.g. Euclid measurements for stage 4 and e.g. KiDS for stage 3.

is similarly done in [22]. The parameters characterizing the noise levels are thus beam width, σ and polarization white noise, Δ_P. Galaxy lensing is determined by measuring lensing shear (see appendices A and D). The noise in this measurement is dominated by scale independent shot noise and has associated noise power spectrum $N_l^{\rm shear} = \sigma_{\rm rms}^2/n_g$. n_g is the amount of galaxies observed per unit angle. The noise power spectrum for the lensing potential then equals

$$N_l^{\text{lens. potential}} = \frac{(l-1)l(l+1)(l+2)}{4} N_l^{\rm shear}.$$

For parameter constraints we use stage 4 noise levels.

The redshift distribution of the observed galaxies is commonly parameterized as [4]

$$n(z) \propto z^a \exp\left[-\left(\frac{z}{z_0}\right)^b\right].$$

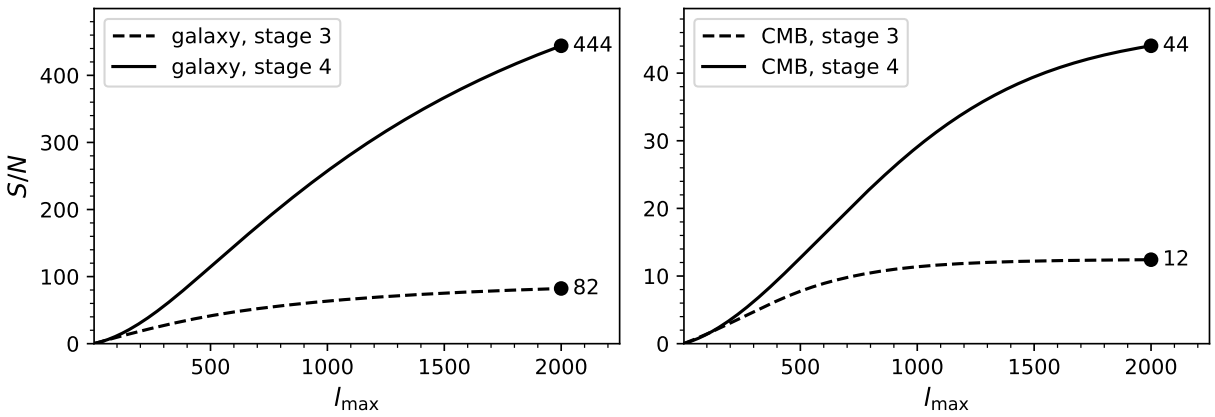

Figure 3: Signal to noise ratios for galaxy lensing (dashed) and CMB lensing (non-dashes) power- (in red) and bispectra (in blue). The x-axis labels the maximum multipole moment measured up to, starting from $l_{\min} = 2$.

We choose the parameter combination $a = 2$, $b = 3/2$ and $z_0 = 0.64$ which is similar to the expected distributions of Euclid, (which will probe primarily in the 0.2 - 2.6 redshift range [10]) and the LSST mission (which has $a \approx 2$, $b \approx 1$, and $z_0 \approx 0.3$ from predictions for the obtained data [15]).

4 Results

4.1 SNR

Lensing power spectra are well detectable in nearly all cases. The signal to noise ratios of the CMB and galaxy lensing bispectra v.s. the maximum multipole moment measured can be found in figure 3. Shear bispectra can be measured well by both stage 3 and stage 4 experiments, while CMB lensing is only semi detectable by a stage 3 experiment but well detectable by stage 4 experiments.

4.2 Parameter Constraints

Parameter constraints for the full set of Λ CDM parameters are shown in figure 5. The combination H_0, σ_8, and Ω_m is particularly well constrained, constraints for these parameters alone (i.e. marginalized over all other parameters) are found in figure 6.

5 Discussion and conclusion

For stage 4 surveys weak lensing matter and power spectra can all be measured with high significance. Additionally, parameter constraints are significantly improved by including bispectrum

Par	CMB + Gal Powersp	CMB + Gal Bisp	CMB Power- + Bisp	Gal Power- + Bisp	CMB + Gal Power- + Bisp
H_0	102.87	1.94	9.63	5.22	0.94
$\Omega_b h^2$	234.33	21.39	25.53	20.30	13.50
$\Omega_c h^2$	127.06	2.43	3.96	3.13	1.42
n_s	25.44	1.94	3.25	3.82	1.51
m_ν	3121.97	307.15	384.96	277.55	178.07
A_s	69.24	6.39	7.96	8.44	4.45
w_0	103.74	2.90	23.14	13.87	2.33
σ_8	31.82	3.85	9.16	4.56	1.84
S_8	37.67	2.08	2.52	2.27	1.14
Ω_m	172.99	5.65	27.29	14.45	3.57
$\sigma_8 \Omega_m^{0.25}$	32.15	2.65	2.82	1.99	1.29

Figure 4: Parameter constraints in percentage of the fiducial values for different combinations of weak lensing information. Below the double line are constraints for derived parameters.

information in nearly all cases. This falls in line with work by Toshiya Namikawa [22], where a 33 percent and 35 percent improvement was found for m_ν and w_0 by measuring the CMB ,lensing bispectrum in addition to the powerspectrum. In particular, from the confidence ellipses it can be seen that these improvements do not just come from additional information, but also because the bispectrum has different (approximate) parameter degeneracies compared to the power spectrum and thus they synergize when combined together.

There are a number of limitations in this work. The most obvious is that the fitting formula used for the nonlinear matter bispectrum is not very accurate, only up to about 10 percent. Additionally, certain parameters that affect nonlinear large scale structure, such as neutrino masses, likely change the fitting parameters of the bispectrum when varied. This is currently not taking into account, making the derivatives less accurate. Another limitation is taking into account full sky effects. We assumed throughout this paper that surveys would measure multipoles as low as $l = 2$, however our analytical formulas to calculate lensing spectra use the Limber approximation, which is only really accurate after $l = 50$. Not using this approximation would make the calculation more complicated due to requireing knowledge of the uneeven time matter power and bispectra and computationally much longer due to having to evaluate a double integral. With the current methods it would thus not be feasible to calculate Fisher matrices without employing the Limber approximation, even if we would be able to calculate the unequel time matter spectra. Perhaps methods used in [8] could be used to solve this problem. Additionally, to calculate the Fisher matrices within a managable timeframe, the derivative of the lensing spectra with respect to cosmological parameters was done using a central difference formula, introducing errors of at most a few percent (CHECK EXACT VALUE LATER) (see appendix E for further discussion) and functions such as the matter power spectrum, fitting parameters of the matter bispectrum, etc. were approximated using pregenerated data and interpolation, also introducing at most a few percent of error. Currently these errors are not significant because this paper only aims to give a rough / qualitative understanding of how usefull CMB and galaxy weak lensing spectra are, however if a similar calculation is done aiming to give precise quantitative results, these factors will need to be looked at again and improved. Furthermore, the current models for calculating lensing noise are on the basic side. Analysing real life data requires a better understanding of underlying systematics. For instance, determining the redshift distribution of galaxies is well known to be a difficult process (CITE SOMETHING HERE) so these errors would have to be taken into account as well. A better estimator can also be used. For example, the iterative estimator developed in CITE leads to a significantly better signal to noise for the CMB lensing bispectrum, as shown in [22]. Finally, for the covariance of the spectra estimators the Gaussian approximation was used, meaning we ignored any contributions not coming from standard Wick contractions, see appendix C. A next step could thus be to take these additional contributions into account, which could perhaps be done by running N body simulations and ray

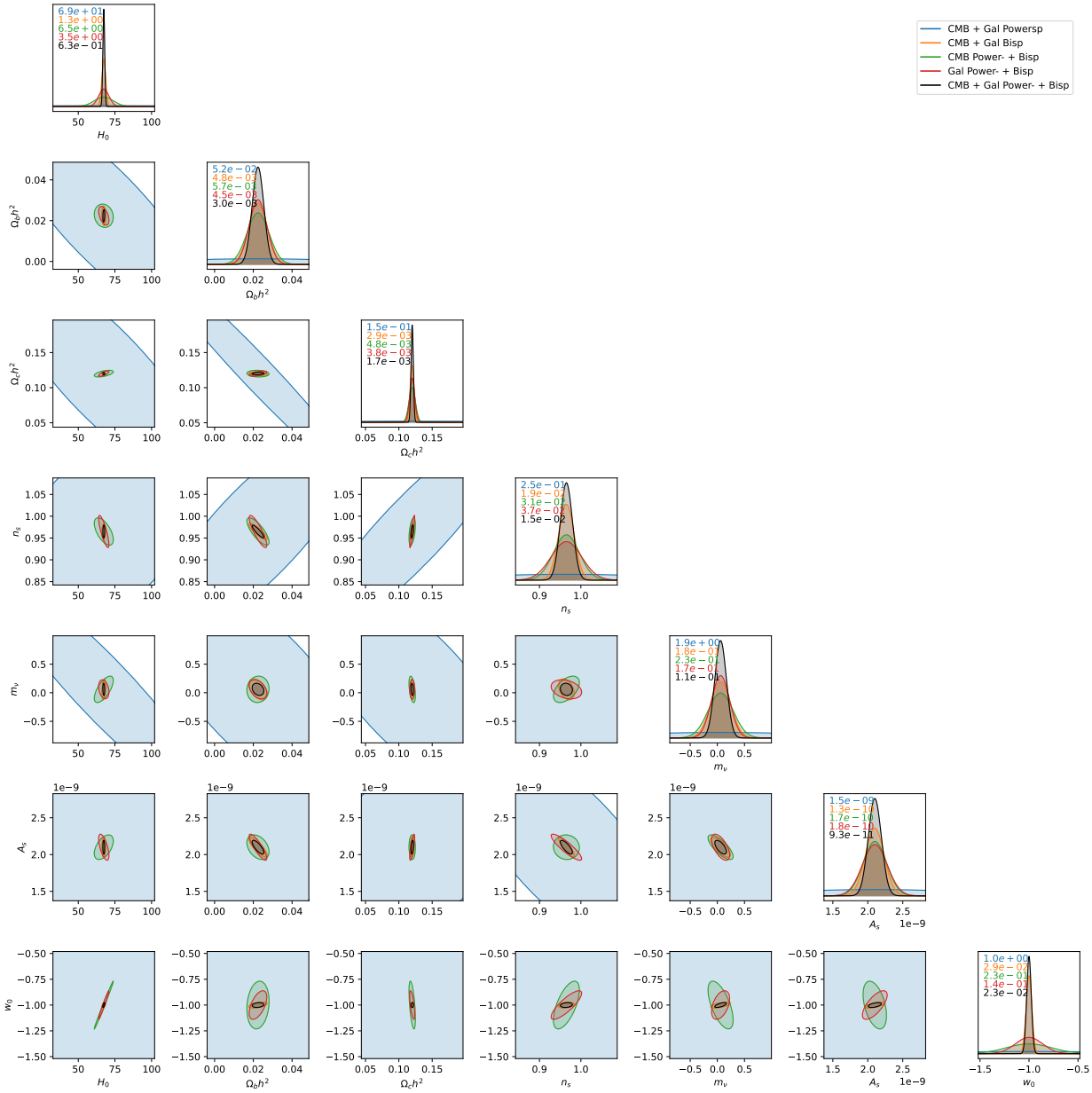

Figure 5: Parameter constraints and confidence ellipses for ΛCDM model as well as neutrino mass and dark energy equation of state parameter. Using "stage 4" noise with multipole range from 2 to 2000. Different weak lensing information combinations considered. No priors used. The confidence ellipses are for 1σ certainty. They show approximate degeneracies in the information gained from a survey if they are "stretched". When the information of ellipses with degeneracies in different directions is combined, the degeneracies are removed and the constraints typically becomes much better on the relevant parameters.

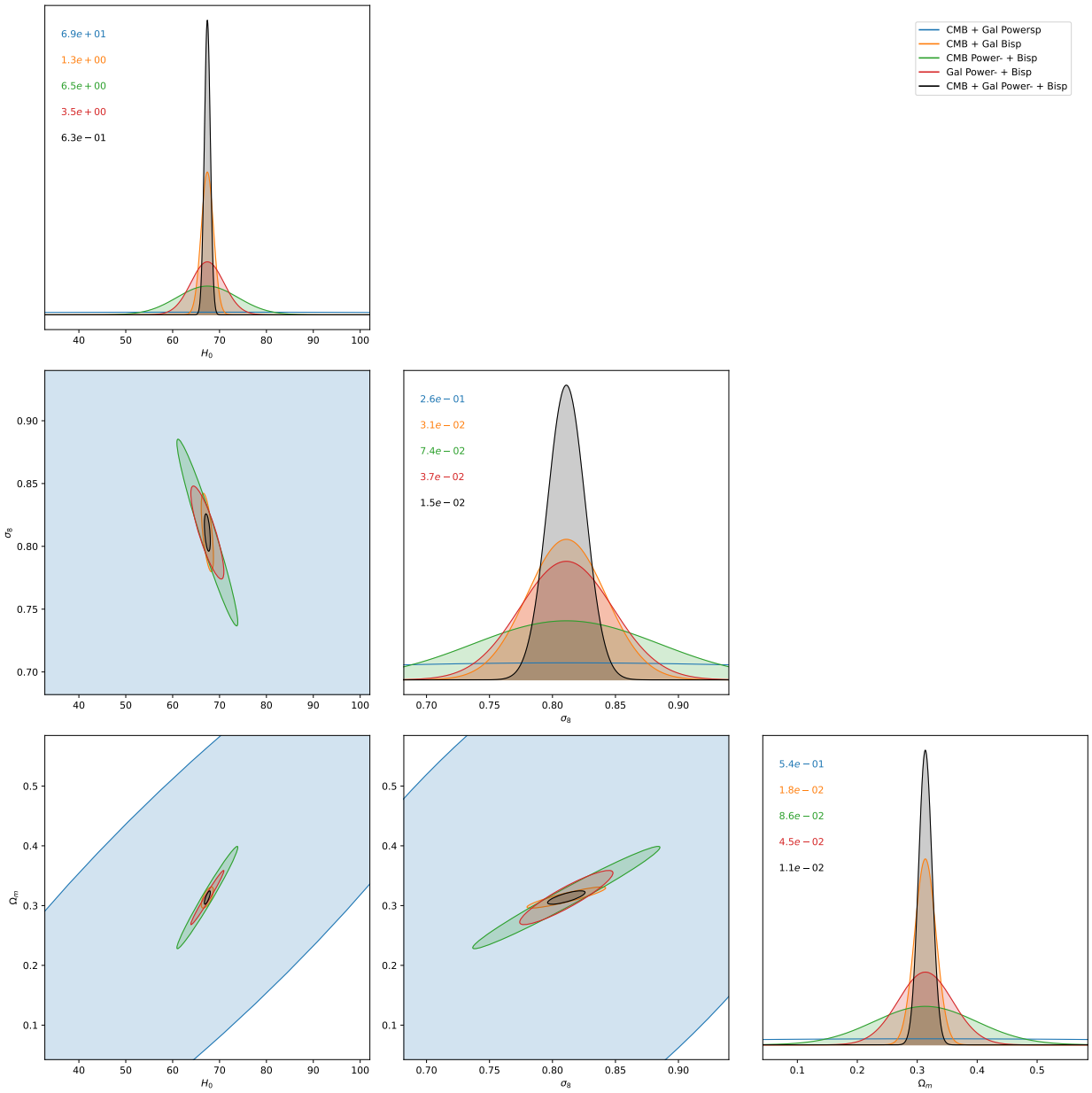

Figure 6: Same as 5, except showing constraints for a set of parameters that can be determined particularly accurately with weak lensing surveys. We chose Hubble's constant, H_0, baryonic + dark matter density, Ω_m, and the root mean square density variation when the matter distribution is smoothed on a scale of 8 megaparsecs, commonly known as σ_8.

tracing simulations. Notably, this could potentially (depending on how accurate the simulations are) also allow us to calculate the lensing spectra much more accurately, i.e. without having to use a fitting formula for the matter bispectrum or Limber approximation.

References

[1] PAR Ade, J Aguirre, Z Ahmed, et al. "The Simons Observatory: science goals and forecasts". In: *Journal of Cosmology and Astroparticle Physics* 2019.02 (2019), p. 056.

[2] N. Aghanim et al. "Planck2018 results: VI. Cosmological parameters". In: *Astronomy and Astrophysics* 641 (Sept. 2020), A6. ISSN: 1432-0746. DOI: 10.1051/0004-6361/201833910. URL: http://dx.doi.org/10.1051/0004-6361/201833910.

[3] D. Bacon, A. Refregier, and R. Ellis. "Detection of weak gravitational lensing by large-scale structure". In: *Monthly Notices of the Royal Astronomical Society* 318 (2000), pp. 625–640.

[4] Matthias Bartelmann and Peter Schneider. "Weak Gravitational Lensing". In: *Physics Reports* 340.4-5 (2001), pp. 291–472. DOI: 10.1016/S0370-1573(00)00082-X.

[5] Matthias Bartelmann and Peter Schneider. "Weak gravitational lensing". In: *Physics Reports* 340 (2001), pp. 291–472.

[6] F. Bernardeau, L. Van Waerbeke, and Y. Mellier. "Weak lensing statistics as a probe of non-Gaussian initial conditions". In: *Astronomy & Astrophysics* 322 (1997), pp. 1–18.

[7] George Casella and Roger L. Berger. *Statistical Inference*. 2nd. Duxbury Pacific Grove, CA, 2002. ISBN: 9780534243128.

[8] Shu-Fan Chen, Hayden Lee, and Cora Dvorkin. "Precise and accurate cosmology with CMB×LSS power spectra and bispectra". In: *JCAP* 05 (2021), p. 030. DOI: 10.1088/1475-7516/2021/05/030. arXiv: 2103.01229 [astro-ph.CO].

[9] Asantha Cooray and Wayne Hu. "Weak Gravitational Lensing Bispectrum". In: *The Astrophysical Journal* 548.1 (Feb. 2001), pp. 7–18. ISSN: 1538-4357. DOI: 10.1086/318660. URL: http://dx.doi.org/10.1086/318660.

[10] Euclid Collaboration: G. Desprez, S. Paltani, J. Coupon, et al. "Euclid Preparation - X. The Euclid Photometric-Redshift Challenge". In: *Astronomy and Astrophysics* 644 (2020), A31. DOI: 10.1051/0004-6361/202039403. URL: https://www.aanda.org/articles/aa/pdf/2020/12/aa39403-20.pdf.

[11] Scott Dodelson and Fabian Schmidt. *Modern Cosmology*. 2nd. Elsevier, 2020. ISBN: 978-0-12-815948-4.

[12] Hector Gil-Marin et al. "An improved fitting formula for the dark matter bispectrum". In: *Journal of Cosmology and Astroparticle Physics* 2012.02 (2012), p. 047. DOI: 10.1088/1475-7516/2012/02/047. arXiv: 1111.4477 [astro-ph.CO].

[13] Henk Hoekstra and Bhuvnesh Jain. "Weak Gravitational Lensing and Its Cosmological Applications". In: *Annual Review of Nuclear and Particle Science* 58.1 (2008), pp. 99–123.

[14] Ž. Ivezić, S. M. Kahn, J. A. Tyson, et al. "LSST: From Science Drivers to Reference Design and Anticipated Data Products". In: *The Astrophysical Journal* 873.2 (2019), p. 111.

[15] Steven M. Kahn, Justin R. Bankert, Srinivasan Chandrasekharan, et al. "LSST System Performance". In: *LSST Science Book, Version 2.0*. Accessed: 2025-02-11. 2009. URL: https://www.lsst.org/sites/default/files/docs/sciencebook/SB_3.pdf.

[16] N. Kaiser, G. Wilson, and G. Luppino. "Large-Scale Cosmic Shear Measurements". In: *arXiv preprint astro-ph/0003338* (2000).

[17] Alba Kalaja, P. Daniel Meerburg, and William R. Pimentel Guilherme L.and Coulton. "Fundamental limits on constraining primordial non-Gaussianity". In: *Journal of Cosmology and Astroparticle Physics* 2021.04 (Apr. 2021), p. 050. ISSN: 1475-7516. DOI: 10.1088/1475-7516/2021/04/050. URL: http://dx.doi.org/10.1088/1475-7516/2021/04/050.

[18] Martin Kilbinger. "Cosmology with cosmic shear observations: a review". In: *Reports on Progress in Physics* 78.8 (2015), p. 086901. DOI: 10.1088/0034-4885/78/8/086901. URL: https://arxiv.org/abs/1411.0115.

[19] R. Laureijs and others (Euclid Collaboration). *Euclid Definition Study Report*. ESA/SRE(2011)12. 2011. arXiv: 1110.3193.

[20] Antony Lewis, Anthony Challinor, and Anthony Lasenby. "Efficient computation of cosmic microwave background anisotropies in closed FRW models". In: *The Astrophysical Journal* 538 (2000), pp. 473–476.

[21] Abhishek S Maniyar et al. "Quadratic Estimators for CMB Weak Lensing". In: *arXiv preprint arXiv:2101.12193* (2021).

[22] Toshiya Namikawa. "CMB lensing bispectrum from nonlinear growth of the large scale structure". In: *Physical Review D* 93.12 (June 2016). ISSN: 2470-0029. DOI: 10.1103/physrevd.93.121301. URL: http://dx.doi.org/10.1103/PhysRevD.93.121301.

[23] Planck Collaboration. "Planck 2018 results. VIII. Gravitational lensing". In: *arXiv e-prints* (July 2018). arXiv: 1807.06210 [astro-ph.CO].

[24] M. Takada and B. Jain. "Cosmological parameters from lensing power spectrum and bispectrum tomography". In: *Monthly Notices of the Royal Astronomical Society* 340 (2003), pp. 580–608.

[25] Max Tegmark. "Cosmic Confusion: Degeneracies among Cosmological Parameters Derived from Measurements of Microwave Background Anisotropies". In: *Monthly Notices of the Royal Astronomical Society* 294.2 (1997), pp. 337–348. DOI: 10.1093/mnras/294.2.337.

[26] L. Van Waerbeke, Y. Mellier, T. Erben, et al. "Detection of correlated galaxy ellipticities from CFH12k VLT data: first evidence for gravitational lensing by large-scale structures". In: *Astronomy & Astrophysics* 358 (2000), pp. 30–44.

[27] L. van Waerbeke et al. "Measurement of cosmic shear three-point correlations in the VIRMOS-Descart survey". In: *Astronomy and Astrophysics* 393 (2002), pp. 369–381. arXiv: astro-ph/0101511 [astro-ph].

A Weak Lensing

A.1 Perturbed Photon Paths

We work in the conformal newtonian gauge and with natural units. Denoting conformal time and conformal radial distance by η and χ, respectively, the perturbed line element in FLRW spacetime is given by

$$\mathrm{d}s^2 = a^2(\eta)((1+2\Psi_N)\mathrm{d}\eta^2 - (1+2\Phi_N)\gamma_{ij}\mathrm{d}x^i\mathrm{d}x^j), \tag{10}$$

where γ_{ij} is the unperturbed line element

$$\gamma_{ij} = \mathrm{d}x^i \mathrm{d}x^j = \mathrm{d}\chi^2 + f_K^2(\chi)(\mathrm{d}\theta^2 + \sin^2\theta \mathrm{d}\phi^2), \tag{11}$$

and $f_K(\chi)$ is the comoving angular diameter distance. We will hereafter only consider a flat universe, so that $f_K(\chi) = \chi$. Weak lensing of a point source can be quantified by looking at the deflection field $\mathbf{d}(\hat{\mathbf{n}}) = \theta_{\mathrm{obs}} - \theta_{\mathrm{true}}$, i.e. the (small) difference between the angle at which we see the object and the angle at which we would see the object had no lensing occured. To first order in Ψ_N and Φ_N, the deflection is given as [11]

$$\mathbf{d}(\hat{\mathbf{n}}) = -2\int_0^{\chi_*} \mathrm{d}\chi \frac{\chi_* - \chi}{\chi_*\chi} \nabla_{\hat{\mathbf{n}}} \Psi(\chi\hat{\mathbf{n}}; \eta_0 - \chi), \tag{12}$$

where Ψ is the Weyl Potential, $\Psi := (\Psi_N - \Phi_N)/2$, and χ_* is the conformal distance to the source. $\nabla_{\hat{\mathbf{n}}}$ is the derivative along the axes orthogonal to the line of sight. The above equation can be written in terms of the lensing potential, ψ, as $\mathbf{d}(\hat{\mathbf{n}}) = \nabla_{\hat{\mathbf{n}}}\psi(\hat{\mathbf{n}})$, with

$$\psi(\hat{\mathbf{n}}) := -2\int_0^{\chi_*} \mathrm{d}\chi \frac{\chi_* - \chi}{\chi_*\chi} \Psi(\chi\hat{\mathbf{n}}; \eta_0 - \chi). \tag{13}$$

If the source is instead distributed over radial distance according to some distribution function $p(\chi)$, with $p(\chi)$ normalized to integrate to 1, the $(\chi_* - \chi)/(\chi_*\chi)$ factor is changed as

$$\frac{\chi_* - \chi}{\chi_*\chi} \to W(\chi) := \int_\chi^\infty \mathrm{d}\chi' p(\chi') \frac{\chi' - \chi}{\chi'\chi}.$$

$W(\chi)$ is then called the window function. In the most general case, the lensing potential is thus given by

$$\psi(\hat{\mathbf{n}}) := -2\int_0^\infty \mathrm{d}\chi W(\chi) \Psi(\chi\hat{\mathbf{n}}; \eta_0 - \chi). \tag{14}$$

The integration limit is sometimes also taken to be the surface of last scattering, as any window function vanishes after that distance. In the case of CMB lensing we can take $p(\chi') = \delta(\chi' - \chi_*)$, in which case the window function reduces to $H(\chi_* - \chi)(\chi_* - \chi)/(\chi_*\chi)$, with $H(\chi)$ the Heaviside step function.

A.2 Convergence and Shear

The magnification matrix is defined as

$$A_{ij} := \delta_{ij} + \frac{\partial}{\partial n_j} d_i(\hat{\mathbf{n}}). \tag{15}$$

This matrix can be decomposed in the following form, which immediately gives us definitions for the **convergence**, κ, **shear**, γ_1 and γ_2, and **rotation**, ω:

$$A_{ij}(\hat{\mathbf{n}}) = \begin{pmatrix} 1 - \kappa - \gamma_1 & -\gamma_2 + \omega \\ -\gamma_2 - \omega & 1 - \kappa + \gamma_1 \end{pmatrix}. \tag{16}$$

At 1st order A is a symetric matrix by definition and ω vanishes, we will ignore it from here on out. Intuitively, A tells you how a small patch in the sky transforms due to lensing. If we change

the unlensed direction of a light source by $\delta\hat{\mathbf{n}}$, then the corresponding change in direction in the lensed image can be calculated as

$$\hat{\mathbf{n}} + \delta\hat{\mathbf{n}} \to \hat{\mathbf{n}} + \delta\hat{\mathbf{n}} + \mathbf{d}(\hat{\mathbf{n}} + \delta\hat{\mathbf{n}}) = \hat{\mathbf{n}} + \mathbf{d}(\hat{\mathbf{n}}) + \delta\hat{\mathbf{n}} + A_{ij}(\delta\hat{\mathbf{n}})_j. \tag{17}$$

For an image on the sky, A_{ij} thus introduces distortion. Note that $|A_{ij}| = (1-\kappa)^2 + \omega^2 - |\gamma|^2 = 1 - 2\kappa + O(\kappa^2, \gamma^2, \omega^2)$. We can thus interpret κ as telling us about the overal magnification of the source. The γ_i represent the area preserving distortion, i.e. stretching and squeezing in a specific direction.

We can relate κ and γ directly to the lensing potential as

$$\kappa = \frac{1}{2}\nabla^2\psi, \quad \gamma_1 = \frac{1}{2}(\partial_{n_1}^2 - \partial_{n_2}^2)\psi, \quad \gamma_2 = \partial_{n_1}\partial_{n_2}\psi. \tag{18}$$

It is shown in appendix D that

$$\gamma := \gamma_1 + i\gamma_2 = \frac{1}{2}\eth_1(\eth_0\psi) \tag{19}$$

where the spin raising operator, $\eth_s$ acts on a spin s function defined on S^2 to create a spin $s+1$ function. $\eth_s$ can be written in spherical coordinates (θ, ϕ) as[2]

$$\eth_s = -\sin^s\theta(\partial_\theta + \frac{i}{\sin\theta})\frac{1}{\sin^s\theta}. \tag{20}$$

In this context a spin s function referes to a function ${}_sf(\theta, \phi)$ that transforms under any rotation of coordinates by picking up a phase factor $e^{is\alpha}$, with α the angle of the rotation, i.e.

$$f'(\theta', \phi') = e^{is\alpha}f(\theta, \phi). \tag{21}$$

Shear is thus a spin 2 function, which can be checked by noting that rotating a galaxy image stretched and squeezed through weak lensing by 180 degrees gives the same stretching and squeezing, i.e. the same shear.

The spherical harmonics are eigenfunctions of ∇^2 and the spin raising and lowering operators. Using this property, the corresponding relations in spherical harmonic space can be shown to be

$$\kappa_{lm} = \frac{l(l+1)}{2}\psi_{lm}, \quad \gamma_{lm} = \frac{\sqrt{(l-1)l(l+1)(l+2)}}{2}\psi_{lm}.$$

B Weak Lensing Statistics

B.1 Lensing Potential Powerspectrum

The lensing potential can be decomposed into spherical harmonics as

$$\psi(\hat{\mathbf{n}}) = \sum_{lm}\psi_{lm}Y_{lm}(\hat{\mathbf{n}}). \tag{22}$$

[2]We use the physics convention for the definition of θ and ϕ here.

On the other hand, consider the decomposition of Ψ in Fourier modes with the Fourier convention $\Psi(\mathbf{x},\eta) = \int \frac{\mathrm{d}^3\mathbf{k}}{(2\pi)^3}\Psi(\mathbf{k},\eta)e^{i\mathbf{k}\cdot\mathbf{x}}$,

$$\psi(\hat{\mathbf{n}}) = -2\int_0^{\chi_*} \mathrm{d}\chi W(\chi)\int \frac{\mathrm{d}^3\mathbf{k}}{(2\pi)^3}\Psi(\mathbf{k},\eta_0-\chi)e^{i\mathbf{k}\cdot\hat{\mathbf{n}}\chi}. \tag{23}$$

We can than relate the multipole modes of ψ to the fourier modes of Ψ through

$$\psi_{lm} = \langle Y_l^m|\psi\rangle = \int \mathrm{d}^2\hat{\mathbf{n}}Y_l^m(\hat{\mathbf{n}})^*\psi(\hat{\mathbf{n}}) \tag{24}$$

$$= -2\int \mathrm{d}^2\hat{\mathbf{n}}Y_l^m(\hat{\mathbf{n}})^*\int_0^{\chi_*}\mathrm{d}\chi W(\chi)\int\frac{\mathrm{d}^3\mathbf{k}}{(2\pi)^3}\Psi(\mathbf{k},\eta_0-\chi)e^{i\mathbf{k}\cdot\hat{\mathbf{n}}\chi} \tag{25}$$

Now define the power spectrum as

$$\langle\Psi(\mathbf{k},\eta)\Psi(\mathbf{k}',\eta')\rangle = \frac{2\pi^2}{k^3}P_\Psi(k,\eta,\eta')\delta(\mathbf{k}+\mathbf{k}'), \tag{26}$$

with η denoting the conformal time. This gives

$$\langle\psi(\hat{\mathbf{n}})\psi(\hat{\mathbf{n}}')\rangle = 4\int_0^{\chi_*}\mathrm{d}\chi\int_0^{\chi_*}\mathrm{d}\chi' W(\chi)W(\chi')\int\frac{\mathrm{d}^3\mathbf{k}}{(2\pi)^6}\frac{2\pi^2}{k^3}P_\psi(k,\eta_0-\chi,\eta_0-\chi')e^{i\mathbf{k}\cdot\hat{\mathbf{n}}\chi}e^{-i\mathbf{k}\cdot\hat{\mathbf{n}}'\chi'}, \tag{27}$$

where we used that $\eta = \eta_0 - \chi$ along the unperturbed photon path (this is known as the Born approximation), with η_0 the time at which the light ray hits earth. We can use the result

$$e^{i\mathbf{k}\cdot\hat{\mathbf{n}}\chi} = 4\pi\sum_{lm} i^l j_l(k\chi)Y_l^m(\hat{\mathbf{n}})^*Y_l^m(\hat{\mathbf{k}}) = 4\pi\sum_{lm} i^l j_l(k\chi)Y_l^m(\hat{\mathbf{n}})Y_l^m(\hat{\mathbf{k}})^*, \tag{28}$$

where j_l is the spherical Bessel function, to rewrite the above equation. Using both versions of the identity above, we immediately get a factor $Y_l^m(\hat{\mathbf{k}})Y_{l'}^{m'}(\hat{\mathbf{k}})^*$ in our integral. We can factor the differential element of $\mathrm{d}^3\mathbf{k}$ into a radial and angular part as $k^2\mathrm{d}k\mathrm{d}^2\Omega_k$, with Ω_k the solid angle, to apply the orthonormality condition of the spherical harmonics. Note that we take the same sequence of steps a number of times in other parts of the derivations of the lensing spectra. We thus obtain

$$\langle\psi(\hat{\mathbf{n}})\psi(\hat{\mathbf{n}}')\rangle = 4(4\pi)^2\sum_{ll'mm'} i^{l-l'}\int_0^{\chi_*}\mathrm{d}\chi\int_0^{\chi_*}\mathrm{d}\chi' W(\chi)W(\chi') \tag{29}$$

$$\times\int\frac{k^2\mathrm{d}k}{(2\pi)^6}\frac{2\pi^2}{k^3}j_l(k\chi)j_{l'}(k\chi')P_\psi(k,\eta_0-\chi,\eta_0-\chi')Y_{lm}(\hat{\mathbf{n}})Y_{l'm'}(\hat{\mathbf{n}}')^*\delta_{ll'}\delta_{mm'}. \tag{30}$$

The angular power spectrum is defined similarly to the power spectrum, i.e.

$$\langle\psi_{lm}\psi^*_{l'm'}\rangle = \delta_{ll'}\delta_{mm'}C_l^\psi. \tag{31}$$

Note that the correlation is independent of m and m'. We can thus read from equation 30 that

$$C_l^\psi = 4(4\pi)^2\int_0^{\chi_*}\mathrm{d}\chi\int_0^{\chi_*}\mathrm{d}\chi' W(\chi)W(\chi')\int\frac{k^2\mathrm{d}k}{(2\pi)^6}\frac{2\pi^2}{k^3}j_l(k\chi)j_l(k\chi')P_\psi(k,\eta_0-\chi,\eta_0-\chi'), \tag{32}$$

which can be simplified to

$$C_l^\psi = \frac{2}{\pi^2}\int_0^{\chi_*}\mathrm{d}\chi\int_0^{\chi_*}\mathrm{d}\chi' W(\chi)W(\chi')\int k^2\mathrm{d}k j_l(k\chi)j_l(k\chi')\frac{P_\psi(k,\eta_0-\chi,\eta_0-\chi')}{k^3}. \tag{33}$$

To further evaluate the integral we will make the Limber approximation. The Bessel functions peak sharply at $l = x^3$, with the peak being increasingly sharp for higher l. Similarly to $\delta(x - x_0)f(x) = \delta(x - x_0)f(x_0)$, we thus take $j_l(k\chi)f(k) \approx j_l(k\chi)f(l/\chi)$. The Bessel functions satisfy an orthogonality condition,

$$\int k^2 \mathrm{d}k j_l(k\chi) j_l(k\chi') = \frac{\pi}{2\chi^2}\delta(\chi - \chi'). \tag{34}$$

In combination with the Limber approximation we thus find

$$\int k^2 \mathrm{d}k j_l(k\chi) j_l(k\chi') f(k) \approx \frac{\pi}{2\chi^2}\delta(\chi - \chi') f(l/\chi). \tag{35}$$

It allows us to write the Limber-approximate angular spectrum as

$$C^\psi(l) = \frac{2}{\pi^2}\int_0^{\chi_*} \mathrm{d}\chi \int_0^{\chi_*} \mathrm{d}\chi' W(\chi)W(\chi')\frac{\pi}{2\chi^2}\delta(\chi - \chi')\frac{\chi^3}{l^3}P_\psi(l/\chi, \eta_0 - \chi, \eta_0 - \chi') \tag{36}$$

$$= \frac{1}{l^3\pi}\int_0^{\chi_*} \chi \mathrm{d}\chi W(\chi)^2 P_\psi(l/\chi, \eta_0 - \chi, \eta_0 - \chi). \tag{37}$$

B.2 Lensing potential bispectrum

The derivation of the bispectrum proceeds similarly to that of the power spectrum. We aim to compute the bispectrum of the lensing potential fields of 3 (possibly distinct sources), ψ_1, ψ_2, ψ_3.

$$\langle (\psi_1)_{l_1 m_1}(\psi_2)_{l_2 m_2}(\psi_3)_{l_3 m_3}\rangle = \prod_i \left(-2\int \mathrm{d}^2\hat{\mathbf{n}}_i (Y_{l_i}^{m_i}(\hat{\mathbf{n}}_i))^* \int_0^{\chi_*} \mathrm{d}\chi_i W_i(\chi_i) \int \frac{\mathrm{d}^3\mathbf{k}_i}{(2\pi)^3} e^{i\mathbf{k}_i\cdot\hat{\mathbf{n}}_i\chi_i}\right)$$
$$\times \langle \prod_i \Psi(\mathbf{k}_i, \eta_0 - \chi_i)\rangle.$$

Defining the bispectrum of the graviational potential as

$$\langle \prod_{i=1,2,3} \Psi(\mathbf{k}_i, \eta_0 - \chi_i)\rangle = (2\pi)^3\delta(\mathbf{k}_1 + \mathbf{k}_2 + \mathbf{k}_3)B^\Psi(\{k_i\}, \{\eta_0 - \chi_i\}),$$

we rewrite the lensing potential bispecrum as

$$\langle (\psi_1)_{l_1 m_1}(\psi_2)_{l_2 m_2}(\psi_3)_{l_3 m_3}\rangle = \prod_i \left(-2\int \mathrm{d}^2\hat{\mathbf{n}}_i (Y_{l_i}^{m_i}(\hat{\mathbf{n}}_i))^* \int_0^{\chi_*} \mathrm{d}\chi_i W_i(\chi_i) \int \frac{\mathrm{d}^3\mathbf{k}_i}{(2\pi)^3} e^{i\mathbf{k}_i\cdot\hat{\mathbf{n}}_i\chi_i}\right)$$
$$\times (2\pi)^3\delta(\mathbf{k}_1 + \mathbf{k}_2 + \mathbf{k}_3)B^\Psi(\{k_i\}, \{\eta_0 - \chi_i\}).$$

Now using equation 28 to rewrite the complex exponential:

$$\langle (\psi_1)_{l_1 m_1}(\psi_2)_{l_2 m_2}(\psi_3)_{l_3 m_3}\rangle$$
$$= \prod_i \left(-2\int \mathrm{d}^2\hat{\mathbf{n}}_i (Y_{l_i}^{m_i}(\hat{\mathbf{n}}_i))^* \int_0^{\chi_*} \mathrm{d}\chi_i W_i(\chi_i) \int \frac{\mathrm{d}^3\mathbf{k}_i}{(2\pi)^3} 4\pi \sum_{lm} i^l j_l(k_i\chi_i) Y_l^m(\hat{\mathbf{n}}_i) Y_l^m(\hat{\mathbf{k}}_i)^*\right)$$
$$\times (2\pi)^3\delta(\mathbf{k}_1 + \mathbf{k}_2 + \mathbf{k}_3)B^\Psi(\{k_i\}, \{\eta_0 - \chi_i\})$$
$$= \left[\prod_i \left(-2\int_0^{\chi_*} \mathrm{d}\chi_i W_i(\chi_i) \int \frac{\mathrm{d}^3\mathbf{k}_i}{(2\pi)^3} 4\pi i^{l_i} j_{l_i}(k_i\chi_i) Y_{l_i}^{m_i}(\hat{\mathbf{k}}_i)^*\right)\right] (2\pi)^3\delta(\mathbf{k}_1 + \mathbf{k}_2 + \mathbf{k}_3)B^\Psi(\{k_i\}, \{\eta_0 - \chi_i\}).$$

[3]Some sources use $x \approx l + 1/2$ instead, which is slightly more accurate for larger scales (low l) and slightly less accurate for smaller scales.

We can write the 3D dirac delta function in terms of spherical harmonics as

$$\delta(\mathbf{k}_1+\mathbf{k}_2+\mathbf{k}_3) = 8\int \mathrm{d}^3\mathbf{x} \prod_{i=1,2,3}\left(\sum_{l_j m_j} i^{l_j} j_{l_j}(k_i x) Y_{l_j}^{m_j}(\hat{\mathbf{k}_i}) Y_{l_j}^{m_j}(\hat{\mathbf{x}})^*\right).$$

This results in

$$\langle(\psi_1)_{l_1m_1}(\psi_2)_{l_2m_2}(\psi_3)_{l_3m_3}\rangle = \prod_i\left(-2\int_0^{\chi_*}\mathrm{d}\chi_i W_i(\chi_i)\int\frac{\mathrm{d}^3\mathbf{k}_i}{(2\pi)^3}4\pi i^{l_i} j_{l_i}(k_i\chi_i)Y_{l_i}^{m_i}(\hat{\mathbf{k}_i})^*\right)$$
$$\times(2\pi)^3 8\int\mathrm{d}^3\mathbf{x}\prod_i\left(\sum_{lm} i^l j_l(k_i x)Y_l^m(\hat{\mathbf{k}_i})Y_l^m(\hat{\mathbf{x}})^*\right)B^\Psi(\{k_i\},\{\eta_0-\chi_i\})$$
$$= (2\pi)^3 8\int\mathrm{d}^3\mathbf{x}\prod_i\left(-2\int_0^{\chi_*}\mathrm{d}\chi_i W_i(\chi_i)\int\frac{k_i^2\mathrm{d}k_i}{(2\pi)^3}4\pi(-1)^{l_i}j_{l_i}(k_i\chi_i)j_{l_i}(k_i x)Y_{l_i}^{m_i}(\hat{\mathbf{x}})^*\right)B^\Psi(\{k_i\},\{\eta_0-\chi_i\})$$

The angular part of the $\mathbf{x}$ integral can be evaluated using the identity

$$\int\mathrm{d}\Omega_{\hat{n}}\,Y^*_{l_1m_1}(\hat{x})Y^*_{l_2m_2}(\hat{n})Y^*_{l_3m_3}(\hat{n}) = (-1)^{m_1+m_2+m_3}\int\mathrm{d}\Omega_{\hat{n}}\,Y_{l_1-m_1}(\hat{n})Y_{l_2-m_2}(\hat{n})Y_{l_3-m_3}(\hat{n})$$
$$= (-1)^{m_1+m_2+m_3}\sqrt{\frac{(2l_1+1)(2l_2+1)(2l_3+1)}{4\pi}}\begin{pmatrix}l_1 & l_2 & l_3\\ 0 & 0 & 0\end{pmatrix}\begin{pmatrix}l_1 & l_2 & l_3\\ -m_1 & -m_2 & -m_3\end{pmatrix}\equiv A_{\mathrm{l}}^{\mathbf{m}},$$

giving

$$\langle(\psi_1)_{l_1m_1}(\psi_2)_{l_2m_2}(\psi_3)_{l_3m_3}\rangle = (2\pi)^3 8A_{\mathrm{l}}^{\mathbf{m}}\int x^2\mathrm{d}x\prod_i\left(-2\int_0^{\chi_*}\mathrm{d}\chi_i W_i(\chi_i)\int\frac{k_i^2\mathrm{d}k_i}{(2\pi)^3}4\pi(-1)^{l_i}j_{l_i}(k_i\chi_i)j_{l_i}(k_i x)\right)$$
$$\times B^\Psi(\{k_i\},\{\eta_0-\chi_i\}).$$

Now applying the Limber approximation again:

$$\langle(\psi_1)_{l_1m_1}(\psi_2)_{l_2m_2}(\psi_3)_{l_3m_3}\rangle = (2\pi)^3 8A_{\mathrm{l}}^{\mathbf{m}}\int x^2\mathrm{d}x\prod_i\left(-2\int_0^{\chi_*}\mathrm{d}\chi_i W_i(\chi_i)\frac{1}{(2\pi)^3}\frac{\pi}{2\chi_i^2}\delta(x-\chi_i)4\pi(-1)^{l_i}\right)$$
$$\times B^\Psi(\{l_i/\chi_i\},\{\eta_0-\chi_i\})$$
$$= (2\pi)^3 8A_{\mathrm{l}}^{\mathbf{m}}\int\chi^2\mathrm{d}\chi\prod_i\left(-2W_i(\chi)\frac{1}{(2\pi)^3}\frac{\pi}{2\chi^2}4\pi(-1)^{l_i}\right)B^\Psi(\{l_i/\chi\},\eta_0-\chi).$$

Finally, we aim to rewrite the above in terms of the angular bispectrum of the lensing potential.

The definition for the bispectrum of any set of randomly distributed spherical harmonic components X_{lm}^k is [9]

$$\langle(X_1)_{l_1m_1}(X_2)_{l_2m_2}(X_3)_{x_3m_3}\rangle = \begin{pmatrix}l_1 & l_2 & l_3\\ m_1 & m_2 & m_3\end{pmatrix}B^{X_1X_2X_3}_{l_1l_2l_3}.$$

Note the independence on m_i, this necesarilly follows from statistical isotropy. If $m_1+m_2+m_3\neq 0$, the associated Wigner-3j symbol vanishes and the bispectrum is set to zero. Also note that in this definition we have immediately generalized to include cross correlation between different fields X_1, X_2, X_3. This is relevant when we look at cross correlations between CMB and galaxy lensing. 6758 Using the above definition and the symmetry property

$$\begin{pmatrix}l_1 & l_2 & l_3\\ -m_1 & -m_2 & -m_3\end{pmatrix} = (-1)^{l_1+l_2+l_3}\begin{pmatrix}l_1 & l_2 & l_3\\ m_1 & m_2 & m_3\end{pmatrix},$$

we find

$$B^{\psi_1\psi_2\psi_3}_{l_1l_2l_3} = (-1)^{l_1+l_2+l_3}\sqrt{\frac{(2l_1+1)(2l_2+1)(2l_3+1)}{4\pi}}\begin{pmatrix} l_1 & l_2 & l_3 \\ 0 & 0 & 0\end{pmatrix}(2\pi)^3 8$$
$$\times\int \chi^2 \mathrm{d}\chi \prod_i \left(-2W_i(\chi,\chi_*)\frac{1}{(2\pi)^3}\frac{\pi}{2\chi^2}4\pi(-1)^{l_i}\right) B^\Psi(\{l_i/\chi\},\{\eta_0-\chi\}),$$

where we were able to drop the $(-1)^{m_1+m_2+m_3}$ factor due to the bispecrum vanishing if that sum doesn't equal 0, as mentioned earlier. When all m_i equal zero, the Wigner 3j-symbol gains a number of useful properties In particular, it vanishes if $l_1+l_2+l_3$ is odd, meaning we can drop the $(-1)^{l_1+l_2+l_3}$ factor. Additionally cancelling common factors then gives

$$B^{\psi_1\psi_2\psi_3}_{l_1l_2l_3} = -\sqrt{\frac{(2l_1+1)(2l_2+1)(2l_3+1)}{4\pi}}\begin{pmatrix} l_1 & l_2 & l_3 \\ 0 & 0 & 0\end{pmatrix} 8\int \frac{\mathrm{d}\chi}{\chi^4} W_1(\chi)W_2(\chi)W_3(\chi)B^\Psi(\{l_i/\chi\},\eta_0-\chi). \tag{38}$$

B.3 Gravitational potential spectra in terms of matter spectra

We can rewrite equations 37 and 38 in terms of the matter spectra instead of the ψ spectra using the poisson equation. This allows us to numerically evaluate these lensing spectra using CAMB. The density contrast is defined as

$$\delta(\mathbf{x}) := \frac{\rho(\mathbf{x})-\bar\rho}{\bar\rho}, \tag{39}$$

and the matter spectra are defined in terms of the fourier transformed density contrast $\delta(\mathbf{k})$ as

$$\langle\delta(\mathbf{k},\eta)\delta(\mathbf{k}',\eta)^*\rangle = (2\pi)^3\delta(\mathbf{k}-\mathbf{k}')P^\delta(\mathbf{k},\eta),$$
$$\langle\delta(\mathbf{k}_1,\eta)\delta(\mathbf{k}_2,\eta)\delta(\mathbf{k}_3,\eta)\rangle = (2\pi)^3\delta(\mathbf{k}_1+\mathbf{k}_2+\mathbf{k}_3)B^\delta(k_1,k_2,k_3,\eta).$$

The mean matter density of the universe, $\bar\rho$ is given as

$$\bar\rho(\eta) = \frac{3\Omega_m H_0^2}{8\pi G}\frac{1}{a(\eta)^3},$$

where $a(\eta)$ is the only time dependent factor on the right hand side. The poisson equation relates Ψ to the density contrast as [11]

$$\nabla^2\Psi(\mathbf{x}) = 4\pi G a^2\left(\frac{3\Omega_m H_0^2}{8\pi G}\frac{1}{a^3}\right)\delta(\mathbf{x}) = \frac{3\Omega_m H_0^2}{2}\frac{1}{a}\delta(\mathbf{x}) \implies \Psi(k,\eta) = -\frac{3\Omega_m H_0^2}{2}\frac{1}{a}\frac{\delta(k,\eta)}{k^2}, \tag{40}$$

where $\Psi(k,\eta)$ and $\delta(k,\eta)$ are functions in Fourier space. For the power- and bispectra we find

$$\langle\Psi(\mathbf{k},\eta)\Psi^*(\mathbf{k}',\eta)\rangle = \frac{2\pi^2}{k^3}C^\Psi(k,\eta)\delta(\mathbf{k}-\mathbf{k}') \implies C^\Psi(k,\eta) = \frac{1}{k}(9\Omega_m^2H_0^4\pi)\frac{1}{a^2}C^\delta(k,\eta),$$
$$\langle\Psi(\mathbf{k}_1,\eta)\Psi(\mathbf{k}_2,\eta)\Psi(\mathbf{k}_3,\eta)\rangle = -(2\pi)^3\delta(\mathbf{k}_1+\mathbf{k}_2+\mathbf{k}_3)B^\Psi(k_1,k_2,k_3,\eta)$$
$$\implies B^\Psi(k_1,k_2,k_3,\eta) = -\frac{1}{k_1^2k_2^2k_3^2}\left(\frac{3\Omega_m H_0^2}{2}\right)^3\frac{1}{a^3}B^\delta(\{k_i\},\eta).$$

Finally, we obtain:

$$\boxed{\begin{aligned} C_l^{\psi_X\psi_Y} &= \frac{9}{l^4}\Omega_m^2 H_0^4 \int_0^{\chi_*} \chi^2 \mathrm{d}\chi a(\eta_0-\chi)^{-2} W_X(\chi) W_Y(\chi) C^\delta(l/\chi, \eta_0-\chi), \\ B_{l_1 l_2 l_3}^{\psi_X\psi_Y\psi_Z} &= \sqrt{\frac{(2l_1+1)(2l_2+1)(2l_3+1)}{4\pi}} \begin{pmatrix} l_1 & l_2 & l_3 \\ 0 & 0 & 0 \end{pmatrix} \frac{27}{l_1^2 l_2^2 l_3^2} \Omega_m^3 H_0^6 \\ &\quad \times \int \chi^2 \mathrm{d}\chi a(\eta_0-\chi)^{-3} W_X(\chi) W_Y(\chi) W_Z(\chi) B^\delta(\{l_i/\chi\}, \eta_0-\chi). \end{aligned}}$$

C Fisher Matrix Analysis

C.1 Determing uncertainty in experimental parameters

The Fisher matrix formalism is used to find a lower bound on the constraints we can place on experimental parameters. It combines the Cramer-Rao Inequality [7] with the assumption that we have unbiased estimators following a gaussian distribution [11]. In particular, denoting the Fisher matrix by $F_{\theta_i\theta_j}$, the parameters as θ_i, and their estimators as $\hat{\theta}_i$, it can be shown that

$$\mathrm{Var}(\hat{\theta}_i) \geq \left(F^{-1}\right)_{\theta_i\theta_i}. \tag{41}$$

In the case of n measurements whose outcomes are realizations of random variables x_i, each with associated mean μ_{x_i}, the Fisher matrix is given as

$$F_{\theta_i\theta_j} := \sum_{p,q=1}^{n} \frac{\partial \mu_{x_p}}{\partial \theta_i}(\tilde{\theta}_k)(\mathrm{Cov}^{-1})_{x_p x_q}(\tilde{\theta}_k)\frac{\partial \mu_{x_q}}{\partial \theta_j}(\tilde{\theta}_k), \tag{42}$$

where Cov is the covariance matrix associated with the random vector $(x_1, ..., x_n)$, $\mathrm{Cov}_{x_p x_q} := \mathrm{Cov}(x_p, x_q)$. The derivative of the mean measurement outcomes and measurement covariances will in general depend on the true, unknown, values of the experimental parameters. We therefore evaluate these quantities with for our best guess of the experimental parameters given some outside information. These are known as the "fiducial" values.

C.2 Fisher matrices for power- and bispectra with multiple tracers

For power spectra, the definition of the Fisher matrix gives

$$F_{\alpha\beta} = \sum_{l_{min}\leq l,l'\leq l_{max}} \sum_{[XY][X'Y']} \partial_\alpha C_l^{XY} \left(\mathrm{Cov}^{-1}\right)_{l,l'}^{XY,X'Y'} \partial_\beta C_{l'}^{X'Y'}.$$

Here the covariance matrix is given as

$$\mathrm{Cov}_{l,l'}^{XY,X'Y'} = \langle \hat{C}_l^{XY} \hat{C}_{l'}^{X'Y'} \rangle.$$

The estimator of a power or bispectrum is the product of the estimators of the appropriate tracers, e.g. $\hat{C}_l^{XY} = \hat{X}(l)\hat{Y}(l)$. The sum over $[XY]$ and $[X'Y']$ denotes a sum over possible tracer combinations *without* counting permutations of tracer configuration. This is because permutations are

not distinct signals, i.e. $\hat{X}(l)\hat{Y}(l) = \hat{Y}(l)\hat{X}(l)$. In fact, if we were to count these permutations as distinct signals we will get identical columns and/or rows in our covariance matrix making inversion impossible:

$$\langle \hat{X}(l)\hat{Y}(l)\hat{X}'(l')\hat{Y}'(l')\rangle = \langle \hat{Y}(l)\hat{X}(l)\hat{X}'(l')\hat{Y}'(l')\rangle, \quad \forall X', Y', l'.$$

To evaluate the covariance matrix we again assume that the estimators are gaussian distributed so that we can apply a wick contraction, as is commonly done [25]. In this case we get

$$\mathrm{Cov}_{l,l'}^{XY,X'Y'} = \frac{1}{2l+1}\delta_{ll'}\left(\tilde{C}_l^{XX'}\tilde{C}_l^{YY'} + \tilde{C}_l^{XY'}\tilde{C}_l^{YX'}\right).$$

Two remarks are in order.

1. By definition
$$\langle X_{lm}X'_{l'm'}\rangle = (2\pi)^3\delta_{ll'}\delta_{mm'}C_l^{XX'},$$
so you can average over the measurements done for different values of m, i.e. $X_{l(-l)}$, $X_{l(-l+1)}$, $\cdots$, $X_{l(l-1)}$, X_{ll}. This results in the $(2l+1)^{-1}$ factor in the power spectrum covariance.
2. The tilde is used to denote the powerspectrum as calculated earlier plus the noise power spectrum, $N_l^{XX'}$, which is the power spectrum of the noise associated with the estimator of the field. This is where experimental noise is incorporated into the calculation.

Under the Gaussian approximation the covariance matrix vanishes except for 3×3 block matrices (in the case of 2 tracers) on the diagonal. The fisher matrix is then

$$F_{\alpha\beta} = \sum_l \sum_{[XY][X'Y']} \partial_\alpha C_l^{XY}\left(\mathrm{Cov}_l^{-1}\right)^{XY,X'Y'}\partial_\beta C_l^{X'Y'}.$$

Cov_l^{-1} here denotes the inverse of the block matrix at l.

Next, we consider the Fisher matrix for bispectra measurements.

$$F_{\alpha\beta} = \sum_{\text{distinct signals}} \sum_{\text{distinct signals prime}} B_{l_1l_2l_3}^{XYZ}\left(\mathrm{Cov}^{-1}\right)_{l_1l_2l_3,l_1'l_2'l_3'}^{XYZ,X'Z'Y'} B_{l_1'l_2'l_3'}^{X'Y'Z'}.$$

Counting only distinct signals requires more care compared to the power spectra. The rule is that $B_{l_1l_2l_3}^{XYZ}$ and $B_{l_1'l_2'l_3'}^{X'Y'Z'}$ are not distinct signals if there exists a permutation σ that simultaniously maps $X'Y'Z'$ to XYZ and $l_1'l_2'l_3'$ to $l_1l_2l_3$. It turns out that we can write a sum over distinct signals explicitly as

$$\sum_{\text{distinct signals}} = \underbrace{\sum_{l_1=l_2=l_3}\sum_{[XYZ]}}_{\text{sum 1}} + \underbrace{\sum_{l_1=l_2\neq l_3}\sum_{[XY]Z}}_{\text{sum 2}} + \underbrace{\sum_{l_1<l_2<l_3}\sum_{XYZ}}_{\text{sum 3}}.$$

With the same definition again for the $[\cdot]$ notation. For example:

$$\{[XY]Z | X, Y, Z \in \{\psi_\kappa, \psi_\gamma\}\} = \{\psi_\kappa\psi_\kappa\psi_\kappa, \psi_\kappa\psi_\gamma\psi_\kappa, \psi_\gamma\psi_\gamma\psi_\kappa, \psi_\kappa\psi_\kappa\psi_\gamma, \psi_\kappa\psi_\gamma\psi_\gamma, \psi_\gamma\psi_\gamma\psi_\gamma\}.$$

It follows to show that the sets that these sums sum over form a partition of the set of all distinct signals. Clearly all 3 sets are pairwise disjoint (no common elements) because of the criteria for the l_i's. To show that their union covers the set of distinct signals, start by considering an arbitrary signal. Its l configuration will trivially correspond to exactly one of the three sums. If it is sum 1, then we are free to permute the XYZ's by virtue of the l's being identical so we will be able to match the XYZ configuration to one of the elements of $\{\{XYZ\}\}$. Similarly, if the l configuration corresponds to sum 2, then we are free to permute the XY configuration to match with one of the elements of $\{\{XY\}Z\}$. The Z value does not matter because any Z value is accounted for. For sum 3 we can argue that we can switch around the order of the l's to satisfy $l_1 < l2 < l3$ and the corresponding XYZ configuration will be accounted for in sum 3 because all XYZ combinations are counted. Finally, it is simple to verify that no distinct signal is counted more than once within each sum.

To calculate the elements of the covariance matrix consider the following. Every element of the Fisher matrix can be seen as an inner product weighted by the inverse covariance matrix. We can choose how we order the vectors[4]. We organize the vectors according to the sum 1, 2, and 3 parts first. Then by l configuration. Within each l configuration we can choose any ordering for the XYZ configurations. The covariance matrix now becomes a block matrix with each block corresponding to an l_i and l_i' configuration. When wick contracting using the gaussian approximation, every block matrix where $(l_1, l_2, l_3) \neq (l_1', l_2', l_3')$ vanishes. It can then be shown that the entries of each block matrix are given as

$$\begin{aligned}(\mathrm{Cov}_{l_1 l_2 l_3})^{XYZ,X'Y'Z'} = \tilde{C}_{l_1}^{XX'}\tilde{C}_{l_2}^{YY'}\tilde{C}_{l_3}^{ZZ'} + \delta_{l_1 l_2}\tilde{C}_{l_1}^{XY'}\tilde{C}_{l_2}^{YX'}\tilde{C}_{l_3}^{ZZ'} + \delta_{l_2 l_3}\tilde{C}_{l_1}^{XX'}\tilde{C}_{l_2}^{YZ'}\tilde{C}_{l_3}^{ZX'} \\ +\delta_{l_3 l_1}\tilde{C}_{l_1}^{XZ'}\tilde{C}_{l_2}^{YY'}\tilde{C}_{l_3}^{ZX'} + \delta_{l_1 l_2}\delta_{l_2 l_3}\left(\tilde{C}_{l_1}^{XY'}\tilde{C}_{l_2}^{YZ'}\tilde{C}_{l_3}^{ZX'} + \tilde{C}_{l_1}^{XZ'}\tilde{C}_{l_2}^{YX'}\tilde{C}_{l_3}^{ZY'}\right).\end{aligned}$$

With our ordering this means that the covariance matrix is again a diagonal block matrix, now with blocks of size 4×4 (sum 1), 6×6 (sum 2), and 8×8 (sum 3).

C.3 Explicit form for inverse covariance matrix

The Fisher matrix above can be significantly simplified and written as

$$F_{\alpha\beta} = \sum_{l_1 \leq l_2 \leq l_3} \frac{\mathcal{P}_{l_1 l_2 l_3}}{6} \sum_{XYZ} \sum_{X'Y'Z'} \partial_\alpha B_{l_1 l_2 l_3}^{XYZ} (\tilde{C}^{-1})_{l_1}^{XX'} (\tilde{C}^{-1})_{l_2}^{YY'} (\tilde{C}^{-1})_{l_3}^{ZZ'} \partial_\beta B_{l_1 l_2 l_3}^{X'Y'Z'}$$

where, in the case of two tracers,

$$C_l := \begin{pmatrix} \tilde{C}_l^{\psi_1\psi_1} & \tilde{C}_l^{\psi_1\psi_2} \\ \tilde{C}_l^{\psi_1\psi_2} & \tilde{C}_l^{\psi_2\psi_2} \end{pmatrix}$$

and $\mathcal{P}_{l_1 l_2 l_3}$ is defined as the number of distinct permutations that can be made with $l_1 l_2 l_3$. This form was, for example, used in [17][5].

[4]The entries are the derivatives of the bispectra

[5]Note that in [17] this is based on a previous equation summing over *all* l_i (so including permutations of each configuration) which is missing a factor of 1/6.

To show that the above is the same as the formula for the Fisher matrix given earlier, first parition the sum in the same way and collect all terms that fit in the different categories.

$$
\begin{aligned}
F_{\alpha\beta} = &\sum_{l_1=l_2=l_3} \sum_{[XYZ]} \sum_{[X'Y'Z']} \partial_\alpha B^{XYZ}_{l_1l_2l_3} \left(\frac{\mathcal{P}_{l_1l_2l_3}}{6} \sum_{d.p.XYZ} \sum_{d.p.X'Y'Z'} (\tilde{C}^{-1})^{XX'}_{l_1} (\tilde{C}^{-1})^{YY'}_{l_2} (\tilde{C}^{-1})^{ZZ'}_{l_3} \right) \partial_\beta B^{X'Y'Z'}_{l_1l_2l_3} \\
&+ \sum_{l_1=l_2\neq l_3} \sum_{[XY]Z} \sum_{[X'Y']Z'} \partial_\alpha B^{XYZ}_{l_1l_2l_3} \left(\frac{\mathcal{P}_{l_1l_2l_3}}{6} \sum_{d.p.XY} \sum_{d.p.X'Y'} (\tilde{C}^{-1})^{XX'}_{l_1} (\tilde{C}^{-1})^{YY'}_{l_2} (\tilde{C}^{-1})^{ZZ'}_{l_3} \right) \partial_\beta B^{X'Y'Z'}_{l_1l_2l_3} \\
&+ \sum_{l_1<l_2<l_3} \sum_{XYZ} \sum_{X'Y'Z'} \partial_\alpha B^{XYZ}_{l_1l_2l_3} (\tilde{C}^{-1})^{XX'}_{l_1} (\tilde{C}^{-1})^{YY'}_{l_2} (\tilde{C}^{-1})^{ZZ'}_{l_3} \partial_\beta B^{X'Y'Z'}_{l_1l_2l_3},
\end{aligned}
$$

where "*d.p.*" stands for "distinct permutations". The entries above are then the entries of the inverses of the block matrices mentioned earlier. This can be checked. For example, for the $l_1 = l_2 = l_3$ sum the multiplication of block matrices corresponding to the same l_i configuration can be written as:

$$
\begin{aligned}
&\sum_{[X'Y'Z']} \left(\frac{\mathcal{P}_{l_1l_2l_3}}{6} \sum_{d.p.XYZ} \sum_{d.p.X'Y'Z'} (\tilde{C}^{-1})^{XX'}_{l} (\tilde{C}^{-1})^{YY'}_{l} (\tilde{C}^{-1})^{ZZ'}_{l} \right) \left(\tilde{C}^{X'X''}_{l} \tilde{C}^{Y'Y''}_{l} \tilde{C}^{Z'Z''}_{l} + \text{perms } X''Y''Z'' \right) \\
&= \frac{\mathcal{P}_{l_1l_2l_3}}{6} \left[\left(\sum_{d.p.XYZ} \sum_{X'Y'Z'} (\tilde{C}^{-1})^{XX'}_{l} (\tilde{C}^{-1})^{YY'}_{l} (\tilde{C}^{-1})^{ZZ'}_{l} \right) \tilde{C}^{X'X''}_{l} \tilde{C}^{Y'Y''}_{l} \tilde{C}^{Z'Z''}_{l} \right] + \text{perms } X''Y''Z'' \\
&= \frac{\mathcal{P}_{l_1l_2l_3}}{6} \sum_{d.p.XYZ} \delta_{XX''} \delta_{YY''} \delta_{ZZ''} + \text{perms } X''Y''Z'' = \frac{\mathcal{P}_{l_1l_2l_3}}{6} \delta_{[XYZ],[X''Y''Z'']} + \text{perms } X''Y''Z'' \\
&= \delta_{[XYZ],[X''Y''Z'']}.
\end{aligned}
$$

The sum over the different wick contractions will similarly cancel with the $\mathcal{P}_{l_1l_2l_3}/6$ factor for the $l_1 = l_2 \neq l_3$ sum. For the $l_1 < l_2 < l_3$ sum the proof is similar as well except no cancellation is required.

The same type of simplification can be made in the Fisher matrix for the power spectrum, though it doesn't offer any significant benefits compared to our current 3×3 block matrix form.

C.4 Signal to Noise Ratio (SNR)

To quantify the detectability of the lensing spectra, we introduce an overal amplitude of our signal, A, with fiducial value 1 as experimental parameter and compute F_{AA}. Obviously, $\partial_A \left(A B^{XYZ}_{l_1l_2l_3} \right) |_{A=1} = B^{XYZ}_{l_1l_2l_3}$, so we find

$$
\left(\frac{S}{N} \right)^2 := F_{AA} = \sum_{XYZ,X'Y'Z'} \sum_{l_1\leq l_2\leq l_3} \frac{\mathcal{P}_{l_1l_2l_3}}{6} B^{XYZ}_{l_1l_2l_3} (\tilde{C}^{-1})^{XX'}_{l_1} (\tilde{C}^{-1})^{YY'}_{l_2} (\tilde{C}^{-1})^{ZZ'}_{l_3} B^{X'Y'Z'}_{l_1l_2l_3}.
$$

The equation for the SNR of the power spectra is identical in form.

C.5 Fisher matrix of power- + bispectra

To compute the Fisher matrix of an experiment measuring both lensing power- and bispectra we are required to compute and invert the full covariance matrix. If we keep assuming that the measurements are close enough to Gaussian to be able to use wick contractions to a good approximation, the full covariance matrix simplifies trivially. The correlation between a power- and bispectrum estimator contains an odd (5) amount of fields and thus always vanishes. We are thus allowed to simply add the Fisher matrices of the power- and bispectra to compute the combined Fisher matrix.

D Shear equals twice spin raised lensing potential

Consider a point on S^2, (r_0, θ_0, ϕ_0), at which we observe some cosmological object. We can then define a set of cartesian coordinates $(\tilde{r}, \tilde{y}, \tilde{x})$ as shown in figure 7.

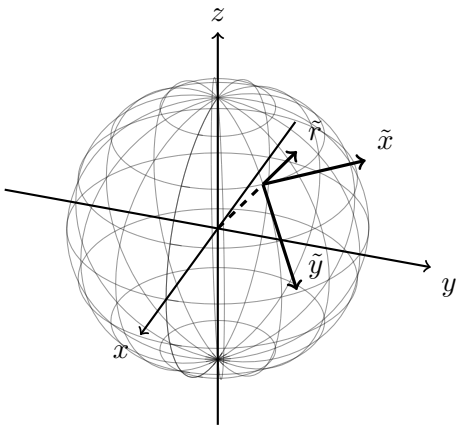

Figure 7: $(\tilde{r}, \tilde{y}, \tilde{x})$ coordinates defined for a point on the unit sphere. These act as ordinary cartesian coordinates but rotated such that, at the associated point on S^2, $\hat{\tilde{r}}$ points straight out of the unit sphere, $\hat{\tilde{y}}$ is parallel to the great arc with constant ϕ and $\hat{\tilde{x}}$ is parallel to the great arc with constant θ. These coordinates are used to define the shear and convergence in terms of the lensing potential.

Note that there it isn't obvious whether to define these coordinates at the point where the lensed light hits S^2 or the unlensed light hits S^2. We will assume that lensing effects are sufficiently weak that either definition works. We can then express the tilde coordinates in terms of spherical coordinates either by applying a rotation matrix or by calculating the r, θ, ϕ derivatives of (x, y, z) coordinates at (r_0, θ_0, ϕ_0) to find $\hat{\tilde{\mathbf{r}}}$, $\hat{\tilde{\boldsymbol{\theta}}}$, and $\hat{\tilde{\boldsymbol{\phi}}}$ and then take inner products. Regardless, we find

$$\tilde{r} = r \sin\theta \cos\phi \sin\theta_0 \cos\phi_0 + r \sin\theta \sin\phi \sin\theta_0 \sin\phi_0 + r \cos\theta \cos\theta_0, \tag{43}$$

$$\tilde{y} = r \sin\theta \cos\phi \cos\theta_0 \cos\phi_0 + r \sin\theta \sin\phi \cos\theta_0 \sin\phi_0 - r \cos\theta \sin\theta_0, \tag{44}$$

$$\tilde{x} = -r \sin\theta \cos\phi \sin\phi_0 + r \sin\theta \sin\phi \cos\phi_0. \tag{45}$$

This gives derivatives

$$\begin{aligned}\frac{\partial}{\partial\theta} =& (r\cos\theta\cos\phi\sin\theta_0\cos\phi_0 + r\cos\theta\sin\phi\sin\theta_0\sin\phi_0 - r\sin\theta\cos\theta_0)\,\frac{\partial}{\partial\tilde{r}}\\ &+ (r\cos\theta\cos\phi\cos\theta_0\cos\phi_0 + r\cos\theta\sin\phi\cos\theta_0\sin\phi_0 + r\sin\theta\sin\theta_0)\,\frac{\partial}{\partial\tilde{y}}\\ &+ (-r\cos\theta\cos\phi\sin\phi_0 + r\cos\theta\sin\phi\cos\phi_0)\,\frac{\partial}{\partial\tilde{x}}.\\ \frac{\partial}{\partial\phi} =& (-r\sin\theta\sin\phi\sin\theta_0\cos\phi_0 + r\sin\theta\cos\phi\sin\theta_0\sin\phi_0)\,\frac{\partial}{\partial\tilde{r}}\\ &+ (-r\sin\theta\sin\phi\cos\theta_0\cos\phi_0 + r\sin\theta\cos\phi\cos\theta_0\sin\phi_0)\,\frac{\partial}{\partial\tilde{y}}\\ &+ (r\sin\theta\sin\phi\sin\phi_0 + r\sin\theta\cos\phi\cos\phi_0)\,\frac{\partial}{\partial\tilde{x}}.\end{aligned}$$

Evaluated at our point of interest we obtain $\partial_\theta = \partial_{\tilde{y}}$ and $\partial_\phi = \sin\theta_0\partial_{\tilde{x}}$. The second order derivatives can then be obtained using the first order derivatives. We can immediately evaluate them at the point to get

$$\begin{aligned}\partial^2_\phi|_{(r_0,\theta_0,\phi_0)} &= -\sin^2\theta_0\partial_{\tilde{r}} - \sin\theta_0\cos\theta_0\partial_{\tilde{y}} + \sin^2\theta_0\partial^2_{\tilde{x}},\\ \partial_\theta\partial_\phi|_{(r_0,\theta_0,\phi_0)} &= \cos\theta_0\partial_{\tilde{x}} + \sin\theta_0\partial_{\tilde{x}}\partial_{\tilde{y}},\\ \partial^2_\theta|_{(r_0,\theta_0,\phi_0)} &= -\partial_{\tilde{r}} + \partial^2_{\tilde{y}}.\end{aligned}$$

Thus, at (r_0, θ_0, ϕ_0),

$$\begin{aligned}\frac{1}{2}\eth_1(\eth_0\psi) &= \frac{1}{2}\sin\theta(\partial_\theta + \frac{i}{\sin\theta}\partial_\phi)(\frac{1}{\sin\theta}(\partial_\theta + \frac{1}{\sin\theta}\partial_\phi))\\ &= \frac{\partial^2\psi}{\partial\theta^2} - \frac{\cos\theta}{\sin\theta}\frac{\partial\psi}{\partial\theta} + \frac{2i}{\sin\theta}\frac{\partial^2\psi}{\partial\theta\partial\phi} - \frac{1}{\sin^2\theta}\frac{\partial^2\psi}{\partial\phi^2} - 2i\frac{\cos\theta}{\sin^2\theta}\frac{\partial\psi}{\partial\phi}\\ &= \frac{1}{2}(\partial^2_{\tilde{y}} - \partial^2_{\tilde{x}} + 2i\partial_{\tilde{x}}\partial_{\tilde{y}})\psi = \gamma_1 + i\gamma_2 = \gamma.\end{aligned}$$

E Numerical derivative

The derivatives with respect to cosmological parameters were taken with a central difference formula, i.e.

$$f'(x) = \frac{f(x+h) - f(x-h)}{2h} + \mathcal{O}(h^2).$$

Each change of the cosmological parameters requires a recalculation of the entire cosmology, making it computationally expensive. For the approximation to be accurate a balance needs to be found between numerical errors for small h and a larger $\mathcal{O}(h^2)$ error for larger h. The h values chosen for each parameter are shown in table 2 and are similar to the values used in [22][6].

To test the accuracy, we vary h by $\pm5\%$ and $\pm10\%$ and plot the relative change in the derivative of the equilateral bispectrum in figure 8. As long as numerical noise doesn't dominate, it can be shown that the relative error in our approximation is approximately 5 times the relative difference

[6] As confirmed during a conversation with the author.

Parameter	Fiducial value	Finite difference (h)
H	67.4	fiducial $\times 0.1$
$\Omega_b h^2$	0.0223	fiducial $\times 0.2$
$\Omega_c h^2$	0.119	fiducial $\times 0.005$
n_s	0.965	fiducial $\times 0.02$
A_s	2.13×10^{-9}	fiducial $\times 0.15$
m_ν	0.06	fiducial $\times 0.15$
w_0	-1	0.06

Table 2: Fiducial cosmological parameters and their finite-difference steps

that taking $h \to h(1 \pm 0.1)$ leads to. We thus conclude that, based on this test, the derivatives are almost always computed with up to one percent of error. The exception is the derivative with respect to neutrino masses, which introduces a larger error.

F Papers compared to

Takada Jain 2005:

- $50 < l < 3000$
- powerspectrum + bispectrum
- galaxy lensing
- $\epsilon = 0.4$, $n_g = 100$, $f_{sky} = 0.1$
- derivative step: 5 percent.
- priors:

$$\sigma(\ln \Omega_B h^2) = 0.01$$
$$\sigma(n) = 0.008$$
$$\sigma(H_0) = 13\sigma(m_\nu) = \infty$$

- constraints obtained by paper:

Quantity	PS	Bisp	PS+Bisp
$\sigma(\Omega_{\rm de})$	0.14	0.13	0.023
$\sigma(\sigma_8)$	0.12	0.12	0.023
$\sigma(w_0)$	4.0	3.6	1.1
$\sigma(w_a)$	20	15	5.1

Planck VII:

- $8 < l < 400$
- powerspectrum only
- cmb lensing
-
- derivative step: 5 percent.
- priors:

$$\sigma(\ln \Omega_B h^2) = 0.01$$
$$\sigma(n) = 0.008$$
$$\sigma(H_0) = 13\sigma(m_\nu) = \infty$$

- constraints obtained by paper:

Quantity	PS	Bisp	PS+Bisp
$\sigma(\Omega_{\rm de})$	0.14	0.13	0.023
$\sigma(\sigma_8)$	0.12	0.12	0.023
$\sigma(w_0)$	4.0	3.6	1.1
$\sigma(w_a)$	20	15	5.1

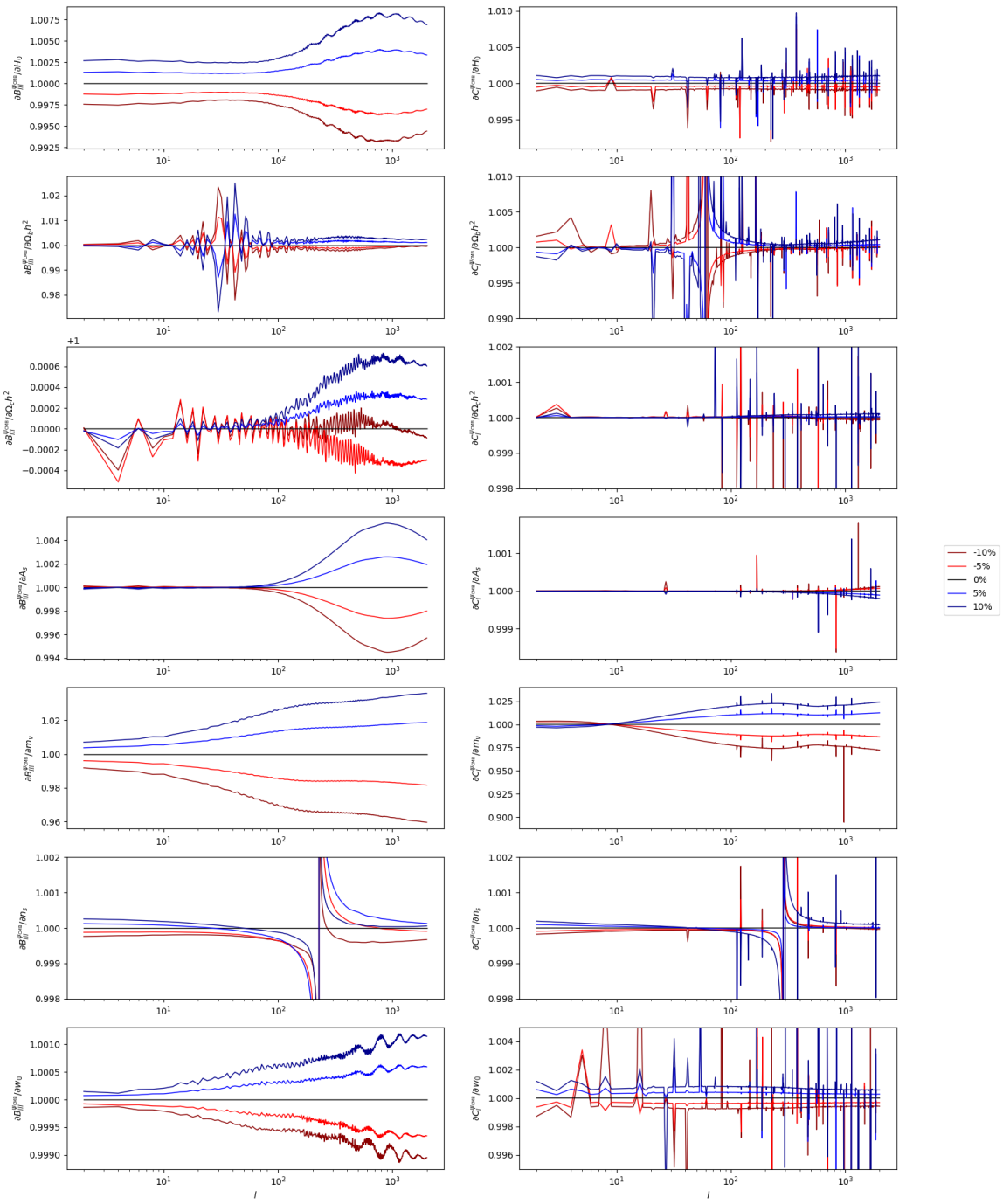

Figure 8: Central difference approximation of derivative of equilateral CMB weak lensing bispectrum (left) and powerspectrum (right) for differences as specified in table 2 as well as for differences 5% and 10% larger and smaller.